The Florida Anthropologist

Volume 65 Numbers 1-2
March-June 2012

Table of Contents

Cover: Artist's depiction of a mastodon kill site and the volunteers of the Wakulla excavations.

Published by the
FLORIDA ANTHROPOLOGICAL SOCIETY, INC.
ISSN 0015-3893

Geoarchaeological Investigations and OSL Dating Evidence in an Archaic and Paleoindian Context at the Helen Blazes Site (8Br27), Brevard County, Florida

W. J. Rink[1], J.S. Dunbar[2], Glen H. Doran[3], Charles Frederick[4], and Brittney Gregory[5]

[1.] School of Geography and Earth Sciences, McMaster University, 1280 Main St.. W., Hamilton, Ontario, Canada L8S 4K1
[2] Department of Anthropology, Florida State University, Tallahassee, FL USA 32306
[3] Department of Anthropology, Florida State University, Tallahassee FL USA, 32306
[4] Department of Geography and Environment, The University of Texas at Austin. 1 University Station A3100, Austin, TX 78712
[5.] Independent Consulting Geoarachaeologist, 2901 FM 1496, Dublin, TX

Introduction

The excavation of the Helen Blazes site (8BR27) between 1949 and 1951 by William Edwards was remarkable for its time, but the assemblage of Archaic and Paleoindian artifacts yielded no materials that could be scientifically dated. This article reports on new excavations at Helen Blazes that were designed to incorporate optically stimulated luminescence (OSL) dating of quartz sand grains and sedimentological studies of the sediment aimed at a better understanding of the depositional context. The new excavations yielded lithic materials with typologies consistent with those found by Edwards (1954). Samples for sedimentological study were analyzed to better understand the depositional context of cultural materials by means of geoarchaeological analysis of site deposits. The OSL ages ranging from about 5,400 to 12,000 years before present are in line with expectation for Archaic to Paleoindian period contexts. However, the sedimentological and geoarchaeological interpretation together with the fine detail of the OSL results suggest that the cultural material at the site was buried by bioturbation and internal reorganization of the deposits rather than normal geological sedimentation following occupation.

The Helen Blazes site is located in peninsular Florida (Figure 1). It is in Brevard County, approximately 27 km west-southwest of the city of Melbourne and about 9 km north-northeast of the headwaters of the St. Johns River. The site lies in the southeast corner of Section 31, Township 29S, R36E, very near Latitude 28.500 N, Longitude 80.750 W (GPS coordinates given in the methods section).

Physiographically, the Helen Blazes site lies 19 km west of the Indian River on the eastern margin of the St. Johns River, 4 km east-southeast of Lake Helen Blazes. Here the St. Johns River floodway is some 6.5 km wide with the lake located in the approximate center of the floodway. The Indian River is a long brackish water lagoon, separating barrier islands and peninsulas (which rarely attain elevations greater than 4 m) from the Atlantic Ocean to its east. The area between the Indian River and Lake Helen Blazes is occupied by the Atlantic Coastal Ridge, which consists of flat, poorly-drained prairies and forests extending to the eastern margin of the St. Johns River floodplain. The terrain west of the Atlantic Coastal Ridge undergoes an imperceptible descent to the Helen Blazes site and continues to descend even more gradually to Lake Helen Blazes, a chain-lake that is part of the St. Johns River (Edwards 1954). Lake Helen Blazes is part of the upper St. Johns River drainage located about 30 km north of the river's headwater at Blue Cypress Lake. Flat, poorly-drained prairies and forests continue west of the St. Johns river basin for 25 to 30 km. Just west of this lies the higher (greater than 30 m above sea level) Osceola Plain (White 1970).

The area is now a flat prairie that still seasonally floods for short intervals. Prior to construction of the Melbourne-Tillman drainage system in 1923 and additional ditching near the site, it was probably a shallow marsh inundated at least part of the year with rainwater and overflow from Lake Helen Blazes. Edwards (1954) noted that with heavy rain the area could be flooded with as much as 1 m of water for short periods. This is still an accurate description and short term flooding is common. The site is positioned on a slight, almost imperceptible, rise on what may be a relic dune or ancient terrace of the St. Johns River. In this region of Florida even slightly elevated areas would have provided some protection during episodes of high water.

Previous Work at Helen Blazes

Earlier work in the immediate vicinity of the site in the 1940s was prompted by the landowner's recovery of megafauna skeletal material from the South Indian Fields site (8BR23; Rouse 1951), which is immediately adjacent to the Helen Blazes site (Figure 2). Excavations peripheral to the main excavations at 8BR23 identified seemingly discrete archaeological deposits that would ultimately be designated as 8BR27, the Helen Blazes site. Edwards, a Columbia University Ph.D. student who had been assisting Rouse and Clarence Simpson (Florida Geological Survey) in their Paleoindian investigations, used the excavations of 1949, 1950, and 1951 as the corpus of his dissertation (Edwards 1954). Edwards' research was conducted with significant attention to the

Figure 1. Location Map showing the Helen Blazes Site in Florida

geological nature of the deposits and the region's geological history. Though his attempts to correlate the depositional history with ancient sea level histories relied mostly on now discarded terminology, his stratigraphic and sedimentological documentation was excellent. Figure 3 provides a diagrammatic explanation of the general stratigraphic situation and correlates descriptions of the sedimentary units to both the major strata (Roman numerals) and subdivisions (Roman letters) and also shows the relative stratigraphic position of diagnostic artifacts recovered by Edwards, as well as the OSL samples and select artifacts recovered from our recent excavations.

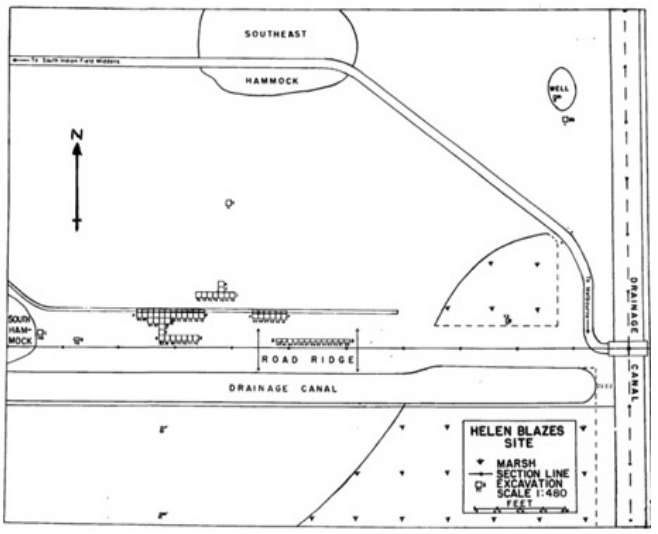

Figure 2. Edwards' original site map of Helen Blazes excavation squares (Edwards 1954:21)

The sedimentary sequence is characterized by marine units comprised of shells, clay, and sand at the base (Strata I and II), clayey to sandy clay units in the central section (Strata IIIA to IIIC), and sandy units at the top (Strata IV to VIIIC).

Edwards reported 7 lanceolate points in his preceramic Strata V and VI and 32 utilized or modified flakes. Four fragments of non-local sandstone 'abraders' were also in Strata V and VI with three possibly attributed to Strata VIII. The unutilized flakes show a similar distribution with all coming from Strata V and VI (Edwards 1954:Table 4). Thus, the majority of the lithics clearly come from the preceramic levels with a heavier concentration in the lower of those levels. All the lanceolate points exhibited grinding of concave basal edges (Edwards 1954). In the 1950s, Paleoindian studies were in their infancy, and many lanceolates were compared favorably with Folsom and Clovis artifacts, which were the first to be described in detail. Thus, Edwards described the lanceolates from Helen Blazes as "Folsom-like" or "Suwanee" [sic].

Prior to the finds at Helen Blazes most of the similar looking lanceolates in the state were from the higher elevations in north-central Florida or in the Tampa area (Simpson 1948:13). Edwards reported looking at two hundred complete and fragmentary lanceolate points in the Simpson and other private collections and most of those had concave bases with basally ground edges that were as straight as specimens D and F (Figure 4; Edwards 1954). He further remarked that "Fish-tail" bases, as in point E of Figure 4, were abundant, while the marked "ears" of point G of Figure 4 would not appear too much out of place in the private collection assemblage. He also noted that true fluting was extremely rare among the central Florida specimens (he saw only two really good examples); a high proportion even lack the large basal thinning spall scars

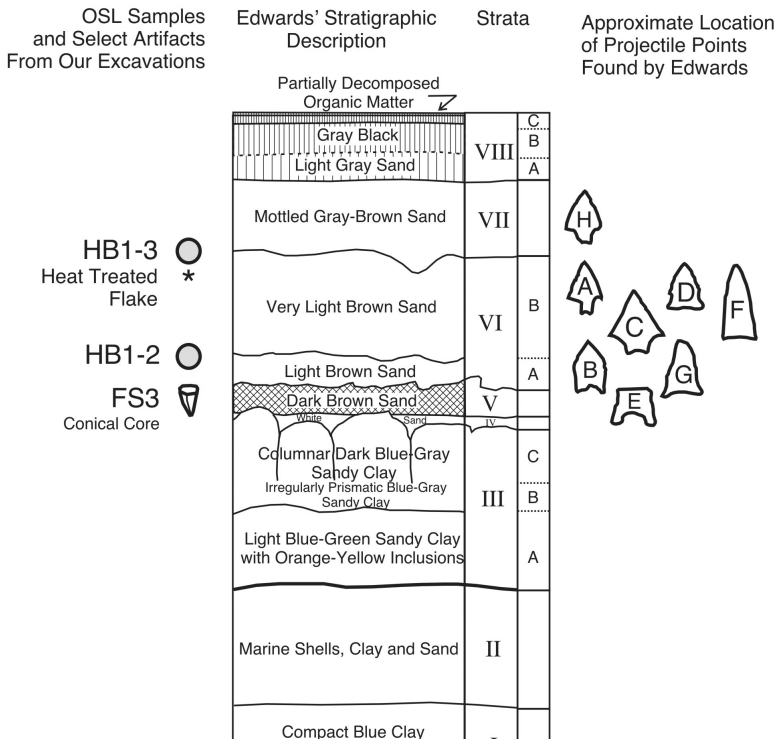

Figure 3. Edwards' original schematic stratigraphy of the Helen Blazes Site (central part of figure; redrawn from Edwards 1954: 25) shown with respect to the approximate stratigraphic position of diagnostic artifacts he recovered. Letters on point icons refer to Edwards (1954:63B) - see also photograph of Figure 4, stratigraphic position of Edward's artifacts derived from Edwards (1954:76B), and the stratigraphic position of the OSL samples and select artifacts collected during the recent excavations.

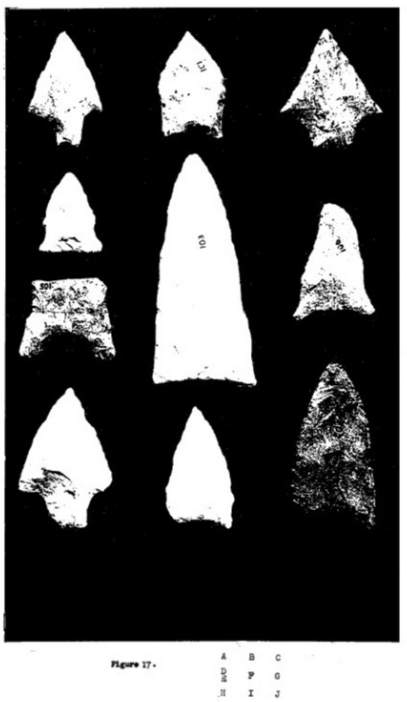

Figure 4. Edwards' original photographs of stone tools found at Helen Blazes (Edwards 1954:63B).

present in some of the Helen Blazes examples. He also noted the workmanship manifest in the eastern Florida specimens he viewed fell well within the broad range of the "Folsom-like" forms. Finally, he reported that "examples almost duplicating points E, F and J are common in central Florida collections" (Edwards 1954:88) and the materials from Helen Blazes showed a good bit of variability. For his time, Edwards' observation that the point assemblage from Helen Blazes was varied is significant and carries important implications that will be discussed below.

Regional Archaeological Context

Many have noted problems with the Florida Paleoindian record: isolated finds, out-of-context materials, few professional excavations, deflated contexts, burial beneath deep sand strata, and materials found in submerged and saturated contexts (Bullen 1969; Daniel and Wisenbaker 1987; Dunbar 1991; Dunbar and Webb 1996; Goodyear and Warren 1972; Knight 2004; Means and Means 2004; Thulman 2006, 2008, 2009). Even so, Thulman (2009:244) proposes Middle Paleoindian materials date between 10,800–10,200 14C B.P. In adjacent areas, Dust Cave in Alabama has yielded an important chronology showing a transition from late Paleoindian lanceolate points and pseudo-notched points beginning around 10,500 ^{14}C B.P. (about 12,540 cal B.P.) to Early Archaic side-notched (Bolen) points after 10,000 ^{14}C B.P. (11,470 cal B.P.) (Sherwood et al. 2004). This chronology, as will be discussed, is equivalent to the OSL date we obtained at 37 cm below datum at Helen Blazes, which is the equivalent of Edward's Level VI that contained the lanceolate and side-notched points (Figure 4). This is also supported by the OSL date from Wakulla Springs (Rink et al. 2012, this volume).

Optically Stimulated Luminescence Dating: Physical Basis and Application

Optical luminescence dating (OSL) utilizes the effects of light exposure on radiation-sensitive defects in the lattice of the quartz mineral. Time dependence arises from a two-stage process in the history of a quartz grain. The first stage is based on the observation that during deposition of quartz sunlight erases previous radiation effects and sets the quartz grain into a zero-age state. The second step involves the burial of the quartz to prevent further light exposure. Once buried natural uranium, thorium, and potassium in the surrounding minerals, as well as cosmic radiation from the sky, introduce energy into the quartz. A small proportion of this energy is trapped

Figure 5. Orthophotograph showing locations of our Shovel Test Units in relation to the geography shown in Figure 4.

inside the quartz grains. This gives rise to a time-dependent accumulation of radiation effects that can be measured in the laboratory.

The total dose of radiation (delivered at a steady rate) experienced in the burial interval is measured in the laboratory by using light to release the stored information during which the quartz is reset to a zero age state, as happened at the time the quartz was exposed to light in nature. Effectively, the quartz acts as a radiation-sensitive photographic film, which must remain in the dark to record an image that can be converted to time (as opposed to photographic film that must be exposed to light to record the image). The time interval of dark storage (burial time) is obtained by establishing the total dose since the last light exposure (called the equivalent dose in laboratory language) and calculating how much dose was acquired in each year of dark burial. The latter quantity is known as the total dose rate and is the amount of dose each year delivered by the uranium, thorium, and potassium in the environment and the amount delivered downward from the sky due to cosmic rays. The burial time is simply the ratio of the dose acquired during dark storage (equivalent dose) to the total dose rate (dose per year). Dose divided by dose per year gives years since burial.

In order for OSL to give an accurate burial age in the archaeological context, the buried grains must remain in their burial location relative to artifacts buried with them. If the buried grains move downward relative to the artifacts, then grains buried at shallower levels may be found with the artifacts, and the grain-age will be too young. Conversely, if buried grains move upward relative to their original burial location, they may arrive into locations with artifacts that were buried at a more recent time in the past. In the latter case, the grain-age will be older than the age of artifact burial.

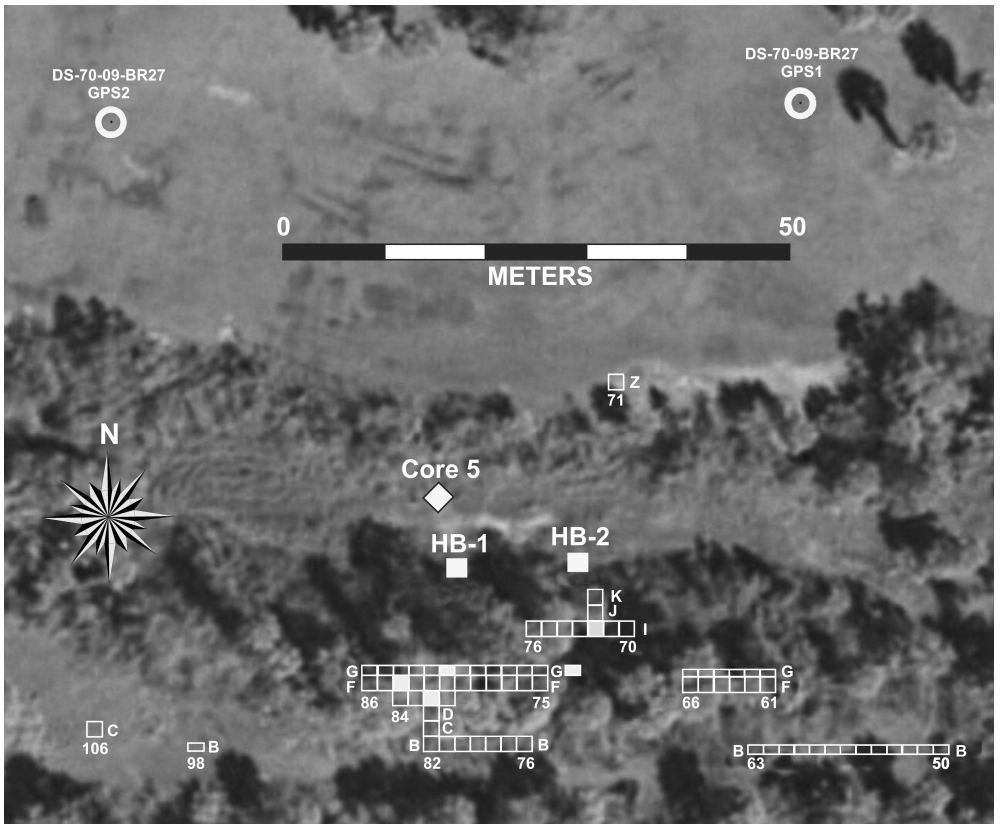

Figure 6. Georeferenced orthophotograph showing our Shovel Test Unit Locations (HB-1, HB-2) and the location of our Core 5. Also shown are the survey control points GPS-1 and GPS 2

Methods and Sample Locations

Archaeological Methods

Edwards' (1954) fieldwork was well documented, and his site map included two control points, one at the southeast corner of T28S, R36E, Section 31 and the other on the South Indian Fields site. These points and the road and canal features illustrated in Edwards' original site map are shown in Figure 2 and can be seen in Figure 5. These details provided a means to relocate precisely the site and previous excavation units. Prior to going to the field, the Edwards site map was georeferenced and superimposed on modern aerial photographs (Figure 6), which allowed scaling distances and directions for the placement of our test pits and tests.We wanted to be close to the Edwards' units so we could confirm the strata he observed and put a series of Geoprobe® cores parallel to the line of Edwards' test unit blocks. We not only confirmed Edwards' stratigraphic observations, but we recovered a number of artifacts from both test units at levels that matched those of Edwards.

Site relocation was conducted using the georeferenced map set, 100-m tapes, a compass, and a handheld GPS unit with an accuracy of 3 to 10 m depending on the time of day and overhead GPS satellite geometry. The site was relocated in this manner. To gain a higher level of survey accuracy the Surveying & Mapping Division of Brevard County Public Works Department lent the services of survey crew using a high accuracy GPS receiver in real-time kinetic mode to pinpoint more precisely our work. Two embossed brass survey plates (Control Point GPS 1 and 2) were set into cement to establish two permanent control points (a baseline) for the site (Figure 6). In turn the Brevard County survey crew set both control points, establishing their horizontal (x, y) and altitude (z) coordinates. The survey crew shot in additional flagged points marking test units and core locations and collected their data in State Plane coordinates, which we converted to UTM, Zone 17 metric coordinate system. The survey data are presented in Table 1.

Our OSL samples were collected in Test Unit 1 (HB1), while the geological data were collected in nearby cores and Test Unit 2 (HB2). The elevation difference of the land surface between the two test units was less than 1 cm. The location of Geoprobe® core 5 is shown on Figure 6. HB1 was located about 8 m northwest of Edwards' square I76, and HB2 was located about 3 m north of his Square K72 (Figure 6). HB1 was excavated using a ¼" screen mesh from 0 to 25 cm, and deeper levels were screened using window screen mesh. HB2 was entirely screened using window screen mesh. A small water pump was used to facilitate screening with the window screen mesh. Artifacts were collected by arbitrary levels in HB1 and natural levels in HB2. All artifacts were recovered from the sand levels of the test units.

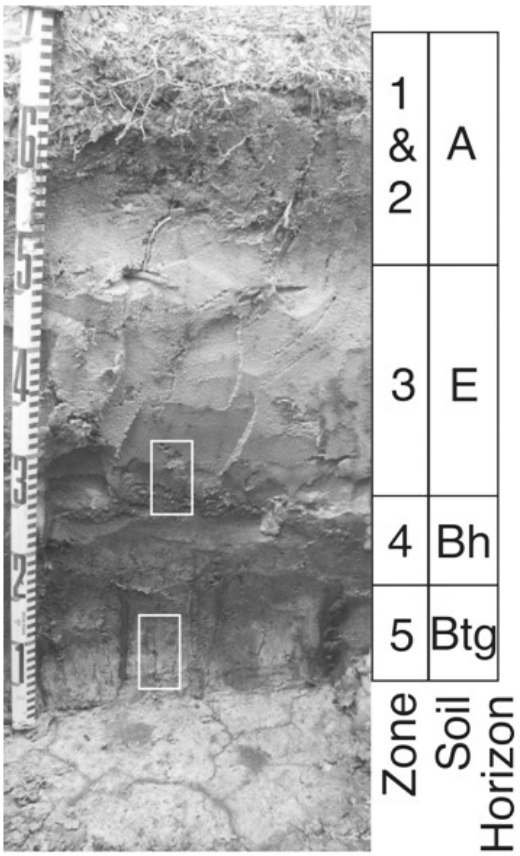

Figure 7. Photograph of Test Unit 2 showing zone designations, soil Horizons, and boxes i(HB2) showing the locations where samples for microphotography were taken as blocks.

The stratigraphic profiles of these tests (Figure 3)

Table 1. GPS coordinates (UTM, Zone 17) and elevations (NAD83-HARN). NE Corner means of the northeast corner of the Shovel Test. GS means ground surface.

Point Name	Easting	Northing	Elevation (m)	Comments
Control Point GPS1	524124.772	3097171.814	4.790	DS-70-09-BR27
Control Point GPS2	524056.638	3097169.992	4.735	DS-70-09-BR27
HB1 Shovel Test	524091.204	3097126.239	4.616	NE Corner GS
HB2 Shovel Test	524102.689	3097126.854	4.618	NE Corner GS
Core 1	524108.545	3097127.685	4.675	Ground Surface
Core 2	524102.852	3097127.355	4.633	Ground Surface
Core 3	524096.567	3097126.972	4.598	Ground Surface
Core 4	524090.593	3097126.804	4.566	Ground Surface
Core 5	524084.377	3097126.617	4.552	Ground Surface

confirmed Edwards' original findings with brown sand levels (Edwards' Strata IV-VIII) resting on top of blue-gray sandy clay (Edwards' Stratum III). The clay level impeded excavations, because it perched rainwater, which seeped into the pits through the porous sand levels and caused the lowest dark brown sand level to collapse into the pit, destroying the lower portion of the profile wall. This prevented successful OSL sampling of the deepest artifact horizon above the blue-gray, sandy clay level.

Geological Methods

The deposits at the site were examined in the field within HB2 (Figure 7), which exposed Edwards' Strata III through VIII. The perched water table precluded clear examination of the lower deposits (Strata I through III), but a more complete stratigraphic section was available by examination of a suite of Geoprobe® cores. A 50-cm long monolith was collected from HB2, and one of the Geoprobe® cores was logged, described, and sampled for physical characterizaton. Two small oriented samples (i.e., tightly wrapped with 'top' and 'bottom' noted) were carved from the profile for petrographic (soil micromorphological) analysis. One was collected from the interface between zones 3 and 4 (Edwards' Stratum VI [the light brown sand] and Stratum V [the dark brown sand]), and a second was collected from near the top of Zone 5 (Edwards' Stratum III [the columnar dark blue-gray sandy clay]).

Bulk samples collected from the monolith and core were analyzed for sediment texture, loss-on-ignition, and calcium carbonate content, and the results are presented on Table 2. Sediment texture was determined on a Beckman-Coulter LS 13-320 laser sizer. Samples were first boiled in concentrated (30 percent) hydrogen peroxide and sodium pyrophospate in order to remove organic matter and disaggregate the clay minerals after which they were subsequently sonicated for 30 seconds prior to analysis. Organic matter was estimated by loss-on-ignition at 450˚C for 2 hours, and calcium carbonate was determined for 17 samples by means of a Chittick apparatus (a device used to measure the calcium carbonate content of soil or sediment by reacting it with hydrochloric acid). The loss-on-ignition values exhibit a slight correlation with the clay content (r=0.60), which suggests that some of these values may reflect structural water loss and therefore may be a poor index of organic matter in clayier deposits. The micromorphological sample was dried at low temperature in an oven and then embedded in polyester resin, after which it was slabbed on a rock saw and a 2 inch by 3 inch large format thin section was prepared. This sample was examined under plane and polarized light on a Leica DMEP petrographic microscope.

Optically Stimulated Luminescence Methods

OSL samples were collected using steel tubes (5 cm diameter, 30 cm long) via slide hammer into the walls of HB1. The locations of the two dated samples HB1-2 and HB1-3 are seen in Figure 8 and in the drawn section (Figure 9). HB1-1 was not collected due to flooding at the time of sampling. The

Figure 8. Photograph showing Shovel Test Unit 1 (HB-1) profiles from which the OSL samples were recovered. HB1-1 was not recovered due to flooding at the time of sampling.

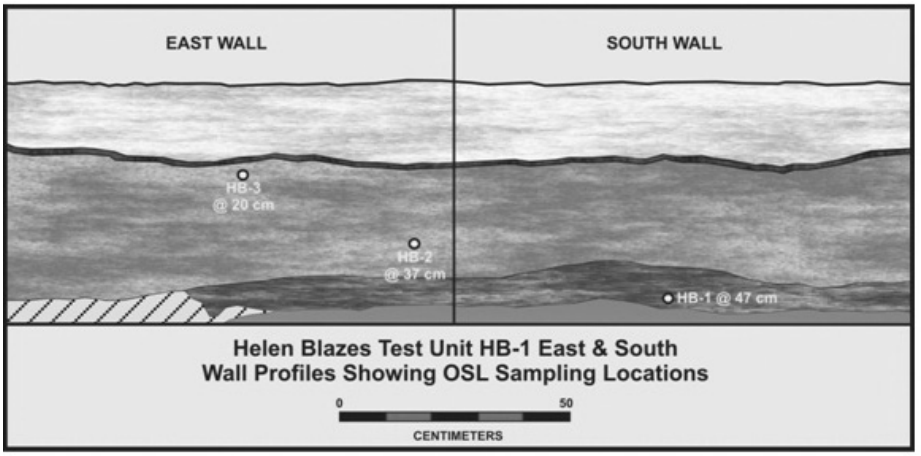

Figure 9. Schematic stratigraphy of Test Unit 2, showing units of varying sediment coloration (light vs. dark).

depths of the OSL samples are given in Table 3. These samples correspond to an upper (HB1-3) and lower sample (HB1-2) in Edwards' Unit VI (Figure 3), though it is possible that the upper sample (HB1-3) might be within Edwards' Unit VII.

All optically-dated samples were processed at the School of Geography and Earth Sciences at McMaster University under UV-filtered subdued orange light. Pure quartz grains were obtained using standard OSL preparation methods that include HCl and H2O2 digestions to remove carbonates and organics, respectively, sieving to obtain desired grain size; heavy liquid separation using lithium polytungstate to remove heavy minerals and feldspars; HF digestion to remove the outer alpha affected layer; a second H2O2 digestion to remove any remaining feldspars and any fluorides that may have formed during the HF digestion; and finally resieving to remove any grains that no longer fall in the desired size range (90-150 microns).

Dose rates were based on neutron activation analysis (NAA) of 232Th and 40K and delayed neutron counting (DNC) analysis of 238U (conducted at the McMaster University Nuclear Reactor). Conversion of radioisotope concentrations to dose rates was done using the data of Adamiec and Aitken (1998) with the addition of 235U dose rates based on its expected natural abundance in relation to 238U (1 part 235U to 137 parts 238U). Untreated subsamples of the original samples were used to determine the elemental concentrations of radioactive 238U, 232Th and 40K (Table 4). NAA/DNC-based dose rates were calculated assuming radioactive equilibrium in the 238U and 232Th decay chains.

Luminescence measurements were conducted on a RISØ OSL/TL-DA-15 reader using blue light LED stimulation (470 nm) and a 7 mm-thick Hoya U-340 filter (270–400 nm). A calibrated 90Sr beta source was used to perform laboratory irradiations. The single aliquot regeneration (SAR) protocol (Murray and Wintle 2000) was conducted on a minimum of 24 aliquots to determine a final equivalent dose (D_E). Quartz grains, between 90-150 microns, were mounted with silicon spray on aluminum discs using a 3 mm and a 1 mm mask and were illuminated for 100 seconds at 125o C. The background (the last 4 s) of the OSL decay curve was subtracted from the "fast" component (first 0.4 s) to determine the samples' luminescence signal. Only aliquots whose recycling ratios were within 10 percent were accepted for equivalent dose D_E determinations. Linear plus exponential fits were made to the dose response data to determine individual D_E values.

Thermal transfer test and dose recovery test were performed to determine the final D_E preheat temperature (Madsen et al. 2005). For both tests, twelve aliquots from each sample were optically bleached by blue light illumination for 40 seconds, followed by a 10,000 second pause and another 40-second illumination. For the dose recovery test, the aliquots were given a known dose. Both tests continued with the standard SAR protocol, except the preheat temperatures varied (160, 200, 240, 280o C), with 3 aliquots from each sample receiving a different preheat temperature. For each sample, the dose recovery test was used to determine which preheat temperature produced a D_E closest to the given dose. Once this preheat temperature was determined the thermal transfer test was analyzed to insure there was no induced charge transfer at that given temperature.

A feldspar contamination check was also performed on each sample to insure purity of the quartz grain separates. An initial DE was estimated by comparing the natural OSL signal (preheat T = 200oC) of three aliquots to the regenerated OSL given by a single dose. A second identical regeneration dose was applied to the same aliquots and the infrared stimulated luminescence signal (IRSL) signal was measured. If a ratio of IRSL to regenerated OSL signal was less than 1% for all aliquots, it is assumed there is no significant feldspar contamination.

Moisture contents were measured in the lab from the recovered sediment and used for the dose rate calculations. The moisture content of the sample can vary during the burial history, thus two estimates were used in the age calculations. Higher average moisture contents yield older ages, while lower average moisture contents yield younger ages. This results from changes in the beta and gamma dose rate that are affected by moisture content.

Table 2. Sedimentological Data for Helen Blazes

	Sample Number	Depth (cm)	Sand (%)	Silt (%)	Clay (%)	Mean (phi)	Median (phi)	Sorting (phi)	Skewness (phi)	Kurtosis (phi)	LOI (%)	USDA Textural Class
Monolith	1	1	92.7	6.21	1.09	2.24	2.20	1.04	0.18	1.27	2.50	Sand
	2	3	95.1	3.97	0.93	2.01	1.98	0.91	0.14	1.21	1.32	Sand
	3	5	94	4.99	1.01	2.00	1.96	1.01	0.19	1.30	1.24	Sand
	4	7	92.5	6.37	1.13	2.12	2.05	1.07	0.26	1.44	1.21	Sand
	5	9	94.4	4.56	1.04	2.00	1.97	0.95	0.17	1.29	0.80	Sand
	6	11	95.3	3.77	0.93	2.02	2.00	0.90	0.13	1.15	0.77	Sand
	7	13	95.5	3.5	1	1.99	1.96	0.89	0.13	1.12	0.39	Sand
	8	15	96.4	2.56	1.04	2.02	2.01	0.83	0.08	1.07	0.15	Sand
	9	17	96.2	2.81	0.99	2.02	2.02	0.85	0.07	1.07	0.16	Sand
	10	19	96.2	2.73	1.07	2.04	2.03	0.84	0.09	1.08	0.14	Sand
	11	21	96.1	2.8	1.1	2.06	2.05	0.86	0.07	1.09	0.05	Sand
	12	23	96.4	2.57	1.03	2.08	2.07	0.83	0.06	1.10	0.10	Sand
	13	25	96.3	2.63	1.07	2.07	2.06	0.84	0.07	1.08	0.17	Sand
	14	27	95.4	3.4	1.2	2.12	2.11	0.89	0.08	1.13	0.12	Sand
	15	29	95.3	3.46	1.24	2.08	2.07	0.90	0.09	1.14	0.13	Sand
	16	31	95.4	3.39	1.21	2.09	2.09	0.88	0.08	1.13	0.04	Sand
	17	33	96.2	2.72	1.08	1.97	1.96	0.86	0.09	1.08	0.09	Sand
	18	35	95	3.73	1.27	2.06	2.04	0.92	0.12	1.17	0.04	Sand
	19	37	93.4	4.93	1.67	2.15	2.13	1.09	0.23	1.61	0.10	Sand
	20	39	90.4	7.21	2.39	2.33	2.27	1.35	0.34	2.19	0.12	Sand
	21	41	86.5	10.44	3.06	2.43	2.28	1.55	0.42	2.27	0.30	Loamy Sand
	22	43	84.9	13.71	1.39	2.63	2.46	1.33	0.30	1.38	1.07	Loamy Sand
	23	45	89.2	9.71	1.09	2.36	2.26	1.19	0.23	1.29	1.71	Sand
	24	47	89.4	9.57	1.03	2.39	2.28	1.16	0.26	1.32	2.16	Sand
	25	49	89.1	9.88	1.02	2.45	2.34	1.14	0.25	1.33	1.52	Sand
	26	50.5	88.7	10.31	0.99	2.45	2.34	1.18	0.25	1.34	1.44	Sand

Table 2 Sedimentological Data for Helen Blazes, continued.

	Sample Number	Depth (cm)	Sand (%)	Silt (%)	Clay (%)	Mean (phi)	Median (phi)	Sorting (phi)	Skewness (phi)	Kurtosis (phi)	LOI (%)	USDA Textural Class
Core	1	2.5	93.4	5.44	1.16	2.13	2.11	1.02	0.19	1.44	0.70	Sand
	2	7.5	94.5	4.38	1.12	2.07	2.05	0.94	0.16	1.28	0.34	Sand
	3	12	96.8	2.26	0.94	1.95	1.93	0.82	0.09	1.05	0.11	Sand
	4	17	96.1	2.82	1.08	2.03	2.02	0.86	0.07	1.08	0.11	Sand
	5	22.5	94.3	4.18	1.52	2.11	2.09	0.97	0.16	1.34	0.05	Sand
	6	27.5	93.8	4.59	1.61	2.14	2.12	1.02	0.19	1.44	0.00	Sand
	7	31.5	94.8	3.83	1.37	2.05	2.04	0.94	0.12	1.20	0.06	Sand
	8	36	93	5.76	1.24	2.11	2.08	1.04	0.20	1.42	0.36	Sand
	9	41	84.3	10.93	4.77	2.65	2.36	1.80	0.49	2.56	1.18	Loamy Sand
	10	44.5	88.6	6.28	5.12	2.49	2.38	1.63	0.44	2.97	1.65	Sand
	11	48	91.4	3.59	5.01	2.47	2.42	1.60	0.37	3.23	1.48	Sand
	12	52.5	93.3	3.46	3.24	2.18	2.13	1.33	0.35	2.24	1.17	Sand
	13	57.5	89.9	5.47	4.63	2.48	2.41	1.60	0.38	2.59	0.87	Sand
	14	63.5	92.6	3.99	3.41	2.39	2.45	1.46	0.06	2.12	0.64	Sand
	15	70	86.7	7.69	5.61	2.53	2.44	1.72	0.41	3.05	0.74	Loamy Sand
	16	75	86.8	7.84	5.36	2.55	2.43	1.65	0.44	3.16	0.76	Loamy Sand
	17	92.5	80.4	14.48	5.12	3.20	2.74	2.03	0.50	2.50	0.76	Loamy Sand
	18	110.5	33.3	60.21	6.49	4.86	4.99	2.57	0.00	0.92	1.00	Silt Loam
	19	115.5	86.6	6.76	6.64	2.17	1.91	1.86	0.58	3.65	1.01	Loamy Sand
	20	120.5	88.4	5.43	6.17	2.06	1.93	1.70	0.50	4.21	0.81	Sand
	21	125.5	92.9	3.08	4.02	1.80	1.79	1.38	0.37	3.54	0.62	Sand
	22	130.5	32.9	40.6	26.5	6.43	6.70	3.17	-0.05	0.63	2.09	Loam
	23	135	69.8	18.6	11.6	4.00	2.46	2.95	0.74	0.98	1.31	Sandy Loam
	24	137.5	83.5	10.88	5.62	2.84	2.42	1.68	0.71	3.74	0.51	Loamy Sand
	25	138.5	69.5	19.4	11.1	4.17	2.81	2.88	0.66	1.21	0.93	Sandy Loam
	26	139.5	83.5	10.88	5.62	3.14	2.77	1.54	0.45	1.34	0.35	Loamy Sand
	27	140.25	69.5	19.4	11.1	4.60	4.02	2.42	0.35	0.79	1.34	Loamy Sand
	28	140.75	83.5	10.88	5.62	3.38	3.02	1.55	0.46	1.30	0.82	Loamy Sand
	29	141.5	69.5	19.4	11.1	3.30	2.81	1.84	0.47	1.50	1.09	Sandy Loam
	30	143.5	74	17.03	8.97	3.95	2.74	2.58	0.70	1.22	0.85	Sandy Loam
	31	146	0	56.8	43.2	8.66	8.62	1.90	0.03	0.99	16.62	Silty Clay
	32	147.5	80.5	12.51	6.99	3.28	2.65	1.95	0.72	2.87	15.46	Loamy Sand
	33	150.5	69	20.4	10.6	4.28	3.05	2.70	0.67	1.30	12.18	Sandy Loam
	34	154	76.2	15.4	8.4	3.67	2.96	2.17	0.66	2.26	11.50	Sandy Loam
	35	159.5	69.3	20	10.7	4.28	3.12	2.65	0.68	1.33	1.09	Sandy Loam

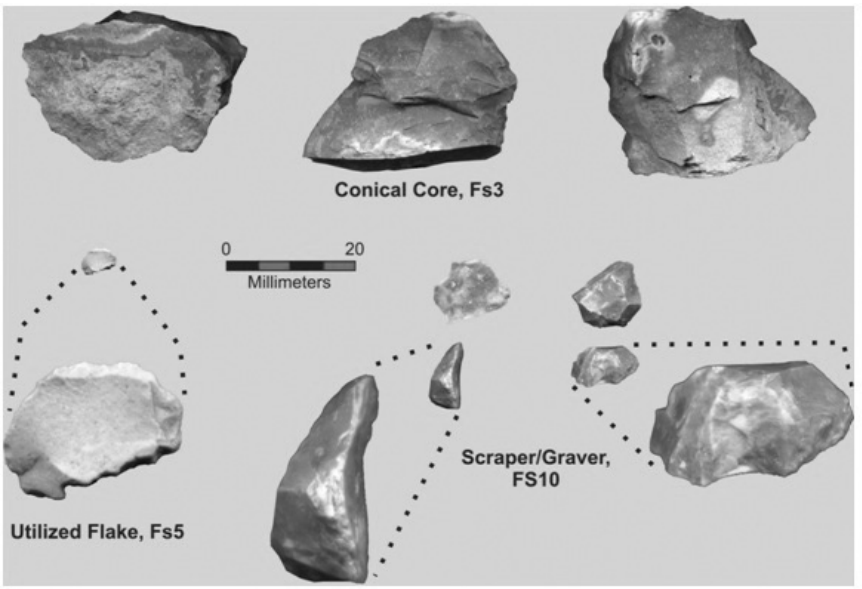

Figure 10. Photographs of tools recovered in our excavations (compare with Table 5).

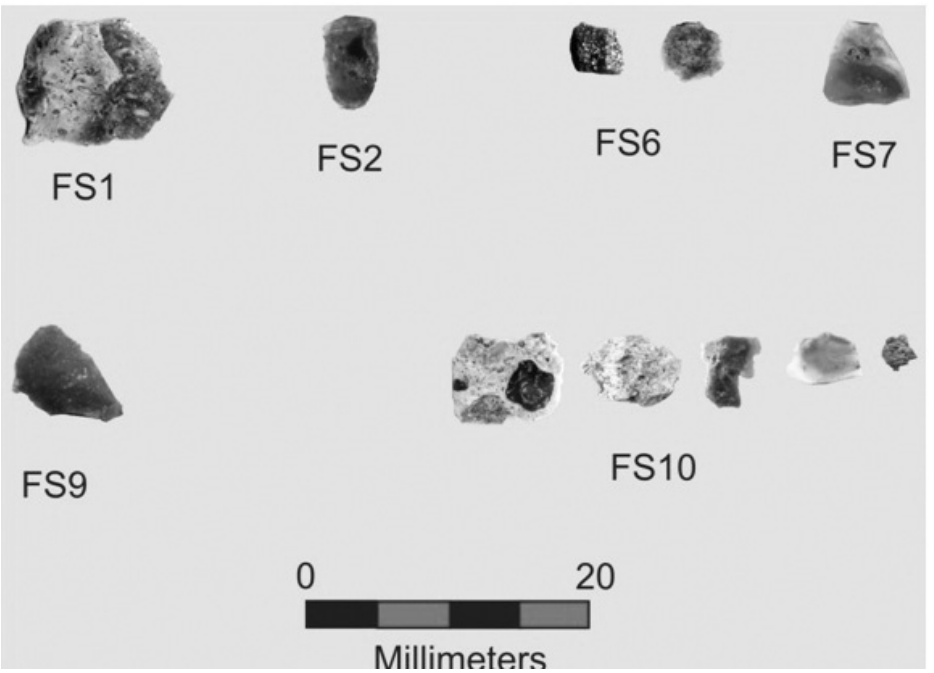

Figure 11. Photographs of flakes recovered in our excavations (compare with Table 5). FS1 is the heat-treated flake.

Table 3. Dose Rate and Optically Stimulated Luminescence (OSL) Age Results for Helen Blazes.

Sample	Depth (cm)	Moisture (%)	Minimum Age Model D_E (Gray) +/- 1 sigma max value	Cosmic Dose Rate (1 x 10^{-6} Gray per year)	Beta Dose Rate (1 x 10^{-6} Gray per year)	Gamma Dose Rate (1 x 10^{-6} Gray per year)	Total Dose Rate (1 x 10^{-6} Gray per year)	OSL Age Minimum Age Model (ka)
HB1-3	17.5-22.5	7	3.5 +/- 0.2	258 +/- 10	163 +/- 12	167 +/- 12	599 +/- 18	5.8 +/- 0.4
HB1-3		30		258 +/- 10	134 +/- 10	140 +/- 10	532 +/- 14	6.5 +/- 0.5
HB1-3 Total Age Range								5.4 to 7.0 ka
HB1-2	34.5 – 39.5	7	5.6 +/- 0.8	238 +/- 10	145 +/- 12	205 +/- 21	598 +/- 24	9.4 +/- 1.4
HB1-2		30		238 +/- 10	119 +/- 10	171 +/- 18	539 +/- 20	10.4 +/- 1.6
HB1-2 Total Age Range								9.0 to 12.0 ka

Table 3. Footnotes

1. Beta and Gamma Dose rates determined using ^{238}U, ^{232}Th and K concentrations determined using delayed neutron counting (^{238}U) and instrumental neutron activation analysis (^{232}Th and K) at the McMaster University Nuclear Reactor. Conversion to dose rates were done assuming equilibrium in the ^{238}U and ^{232}Th decay chains. Conversions were done assuming that ^{235}U was present in its expected natural ratio of 1 part ^{235}U to 137 parts ^{238}U. Dose rate conversion data were obtained from Adamiec and Aitken (1998). Total dose rates include assumed quartz internal ^{238}U and ^{232}Th values from Rink and Odom (1991) of ^{238}U = 0.0665 ppm and ^{232}Th = 0.1135 ppm. These values yielded dose rates of 8.6 +/- 2.2 and 1.9 +/- 0.4 x 10^{-6} Gray per year respectively, using an alpha efficiency factor of 0.04. Concentrations of ^{238}U, ^{232}Th and K used to calculate the beta and gamma dose rates were HB1-3 = 0.6 +/- 0.1 ppm , 1.92 +/- 0.13 ppm and 0.0773 wt.% respectively. ^{238}U, ^{232}Th and K concentrations for HB1-2 were 0.5 +/- 0.1 ppm, 1.92 +/- 0.13 and 0.0675 wt% respectively. For HB1-2 we were able to measure the in-situ gamma dose rate, rather than using sediment radioactivity data; the in-situ dose rate is reported in the table and used to calculate the ages for that sample. Age results and dose rate data were obtained using the software ANATOL provided by N. Mercier, which uses cosmic dose rate calculations based on Prescott and Hutton (1988). As-found moisture contents were between the 7 and 30% estimates used here to bracket time averaged moisture.

Table 4. Concentrations of radionuclides in Helen Blazes OSL samples

Sample	^{238} Uranium (ppm)	^{232} Thorium (ppm)	Potassium (wt. %)
HB1 -3	0.6 +/- 0.1	1.92 +/- 0.13	0.0773 +/- 0.0030
HB1 -2	0.5 +/- 0.1	1.92 +/- 0.13*	0.0675 +/- 0.0003

Results

Archaeological Results

The two one-meter square test units at the Helen Blazes (HB1 and HB2) yielded 14 lithic artifacts, specifically 3 tools and 11 tool maintenance debitage flakes. Their characteristics are given in Table 5 and illustrated in Figures 10 and 11. This is not a large number of artifacts, though they are informative. The relative position of two of the artifacts we collected, Edwards' major finds, and the locations of the OSL samples are shown in Figure 3.

The stratigraphic positions of the artifacts recovered indicate two lithic components are present at the site. In the upper component we recovered a single heat-treated flake from the shallowest level of the test units (19 to 20 cm below surface), which is consistent with Middle Archaic and later period sites and corresponds to Edwards' Stratum VIII where he recovered stemmed-Archaic points. The lower component produced a conical core tool (FS 3.1 at 52 cm below surface) and a graver (FS 10.1 at 30-40 cm below surface). Although they are not diagnostic, these fit nicely with similar Paleoindian to Early Archaic tools (Daniel and Wisenbaker 1987; Dunbar and Vojnovski 2007). The debitage from the lower component (25 cm to 52 cm) are small pressure flakes consistent with both Suwannee and Bolen toolkit manufacture and, in this instance, with careful stone tool maintenance. Generally larger conical core tools, conical cores, and gravers have been recovered at Suwannee point sites such as the Norden site (8GI40) in northern Florida (Dunbar and Vojnovski 2007) and the Suwannee-Bolen point component at the Harney Flats site (8HI507) near Tampa (Daniel and Wisenbaker 1987). Both the Norden and Harney Flats sites are in areas of abundant chert outcrops, and chert conservation measures are absent.

Generally, when chert sources are located near a site, debitage tends to be more abundant and composed of larger and bulkier pieces than when chert sources are more distant from a site. In the latter case, the debitage tends to be less abundant and of smaller size. An accepted inference garnered from the presence of fewer and smaller sized debitage is that people were more careful and less wasteful in their use of chert as they had to walk a long distance to obtain it. The most striking aspect of the debitage assemblage recovered during our investigations is its small size. Had regular ¼-inch screen been used, almost nothing would have been recovered. Window screen was essential for recovering the smaller range of material. Given the exhausted condition of the points recovered by Edwards and the small size of the debitage we recovered, it appears that the occupants of Helen Blazes used and resharpened tools in a way that conserved raw material, which is in agreement with our expectations for a site that is

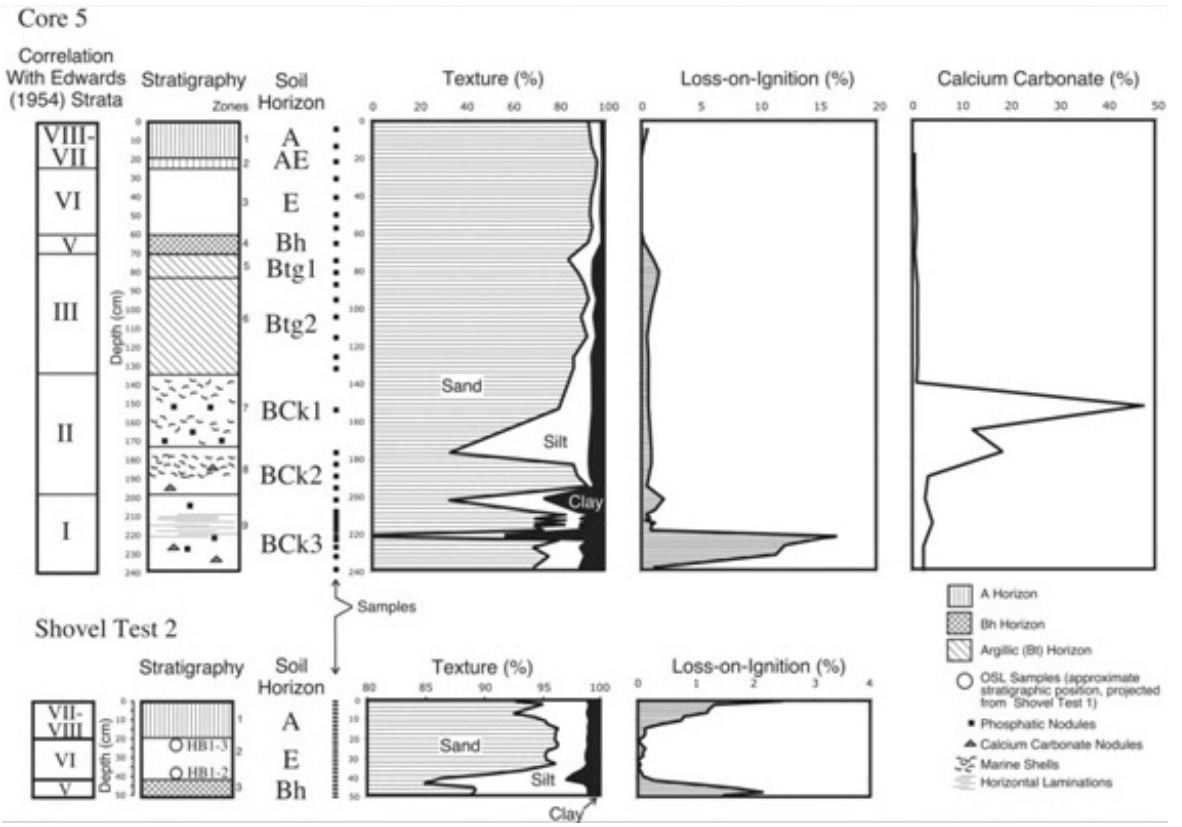

Figure 12. Plot showing the results of the physical properties of Core 5 (upper part) and a monolith collected from Test 2 (lower part) at the Helen Blazes Site. The relative stratigraphic position of the two OSL samples collected from Test 1 are projected onto the stratigraphic drawing of Test 2. Note that the scales for the texture diagrams are not the same on the two drawings, with Test 2 having an expanded scale to show variation present within the unconsolidated sands.

Table 5. Finds List from 2009 Excavation at Helen Blazes, giving depths of finds and type of material. ST identifies the shovel test that object was recovered from. HT – heat treated lithic, NHT-not heat treated

FS No.	Count	Item(s)	Comments
1.1	1	Debitage	HT, Ocala chert, 19-20cm, ST1
2.1	1	Debitage	NHT, Chert?*, 35-40 cm, ST-1
3.1	1	Conical Core tool	NHT, Chert?, 52 cm, ST-1 on top of clay
4.1	1	Plastic shotgun wad	NHT, 0-5 cm
5.1	1	Utilized flake, micro tool	NHT, Ocala chert, 25-30, ST-1
6.1	2	Debitage	NHT, Chert ?, 35-40, ST-1
7.1	1	Debitage	NHT, Chert?, 40-45, ST-1
8.1	NO Artifacts	*1	
9.1	1	Debitage	NTH, Chert?, ~30cm, ST-2
10.1	1	Graver, micro tool	NHT, Chert?, 30-40 cm, ST-2
10.2	2	Debitage	NHT, Peace River Opaline 30-40 cm, ST-2
10.3	3	Debitage	NHT, Chert?, 30-40 cm, ST-2

*Chert? – chert, unidentified source
*1FS numbers assigned in field based on strata prior to excavation and screening

Table 6. Characteristics of Equivalent Dose (D_E) Measurements at Helen Blazes

Sample	Aliquot Diameter (mm)	No. of aliquots accepted	Minimum Age Model D_E (Gray) +/- 1 sigma	p-value	Overdispersion (%)
HB1-3	1	22/48	3.5 + 0.2, - 0.2	0.045	200
HB1-2	1	30/48	5.6 +0.5, - 0.8	0.033	50

distantly located from chert resources.

As shown in Table 5 the origin of identified chert sources were from quarry clusters well over 100 km to the northwest and southeast. Ocala chert outcrops in the Brooksville area about 150 km to the west-northwest of Helen Blazes, although, if one were to assume the most logical movement corridor was the St. Johns River basin, the chert source near Ocala about 175 km to the northwest may have been the nearest source. The occurrence of Peace River opaline chert (about 135 km southwest) is interesting because its practicality as a lithic tool-making resource is marginal at best. Peace River opaline chert is glassy, brittle, and prone to easy breakage compared to the Ocala and other Florida Tertiary cherts. But the real significance of opaline chert is that it is an indication of an early mobility route from the Peace River basin of southwest Florida, where early sites such as Little Salt Springs and Warm Mineral Springs are located, on the south-central Florida East Coast.

Geological Results

Edwards' thorough and detailed description of the Helen Blazes profile is remarkable for its time. The work performed here adds little to his description, but our work does provide the basis for an alternative interpretation of the geological events that led to the formation of these deposits. In general terms, we believe that the sediments preserved at Helen Blazes represent a single marine deposit that has been significantly altered by post-depositional weathering and pedogenesis. Many of the attributes Edwards used to delineate geologic events are post-depositional pedogenic features and not true sedimentary strata. When the profile is closely examined for soil features, it becomes apparent that this profile developed under two sequential climatic phases that were significantly different from each other.

Primary deposition of this marine sediment most likely occurred during the last interglacial (approximately 80,000 to 125,000 years ago). Falling sea levels during the ensuing glaciation and the drier climate and depressed water tables resulted in a freely draining sandy deposit that favored the development of a prominent alfisol within the sediments. During this period of time clay was stripped from the upper part of the profile and concentrated in Zones 5 and 6 (Figure 12) at depth to form an argillic (Bt) horizon (Edwards' Stratum III). Here, "at depth" means this was an internal reorganization at the depths of Zones 5 and 6 (70 to 135 cm below surface) rather than a "normal" geologic sedimentation where sediment is added to the ground surface. Thus, clay was stripped from the top of the profile (Zones 1 to 4) and translocated into what we recognized as Zones 5 and 6. At the same time, detrital calcium carbonate was leached from the upper part of the profile and deposited at depth (i.e., reorganization in Zones 7, 8, and 9 [135 to 240+ cm below surface in core 5], Edwards' Strata I and II) in the form of small calcium carbonate nodules

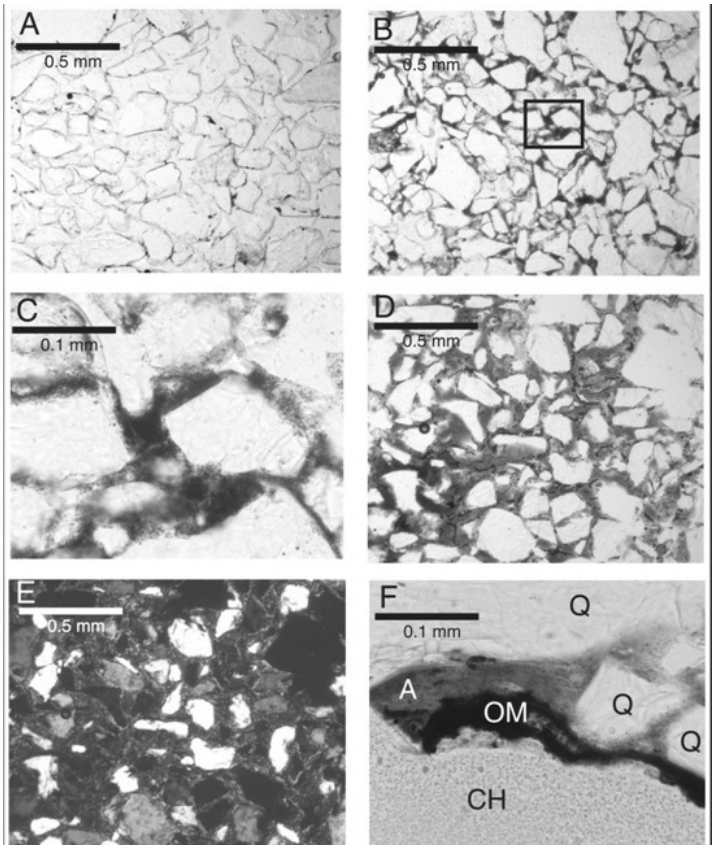

Figure 13. Photomicrographs of selected features of the deposits at the Helen Blazes Site. A. Photomicrograph of the E-horizon (Zone 3) showing the subrounded quartz grains and a lack of grain coats. B. Photomicrograph of the Bh horizon (Zone 4), showing the coats and bridges between grains of illuvial organic matter. Square shows area enlarged in the next photo. C. Same slide as B enlarged to show the coats of organic matter. D. Photomicrograph of the Btg horizon (Zone 5) showing the coats of illuvial clay, light brown color (plane polarized light). E. Same photo as D but shown in cross-polarized light. Note the birefringent clay coats around grains. F. View of superimposed coats along the margin of a channel (CH), where a clay argillan lies adjacent to the quartz (Q) sand grain and is in turn coated by illuvial organic mater (OM) showing the relative sequence in which the coats were deposited.

and calcium phosphate nodules. It is important to note that the depths of these deposits vary across the site. The results of these two processes were the formation of a profile with a sandy upper part (Edwards' Strata V to VIII) and a structured subsoil with increased amounts of clay and silt (Edwards' Stratum III) on top of relatively unweathered sediment to which secondary (pedogenic) calcium carbonate and phosphate were added (Edwards' Strata I and II). The latter retain primary stratification and detrital marine shell and unlike the upper part of the profile still bear a strong resemblance to their appearance immediately following deposition in a marine setting.

The onset of more mesic conditions, rise of the water table and periodic inundation that accompanied deglaciation significantly shifted pedogenesis here in favor of Spodosol development. Spodosols in Florida are created by periods of saturation that submerge acidic leaf litter and lead to the development of strongly acidic organic compounds (chelates) that aggressively attack both the framework minerals as well as grain coats leading to sandy epipedons that are generally very light in color and subsoils with illuvial concentrations of organic matter, iron, and aluminum. It was during this period (most likely the latter half of the Holocene) that Zone 4 (or Edwards' Stratum V; a Bh horizon; see Figure 12) was created, which Edwards correctly identified as a Spodic B horizon consisting of illuvial organic matter. At the same time, the prolonged saturation gleyed the argillic horizon and all of the underlying deposits.

The cultural material within the unstructured sands in the top half meter or so, above Edwards' Stratum III, was most likely deposited on the ground surface and buried by pedoturbation. Prior to the formation of the argillic horizon, pedoturbation by soil fauna (especially insects) would most likely have been in excess of 1 m, but as the argillic horizon became established and started to form an impediment to water movement, their actions would have become concentrated in the loose sands above it. This process was most likely well underway by the time the site was inhabited during the Paleoindian period.

The depths used in the following description relate to the relatively complete profile exposed by coring of the deposit and shown on Figure 12. At the top of the profile is an A horizon (Zone 1) that is a 15 to 18-cm thick gray-light

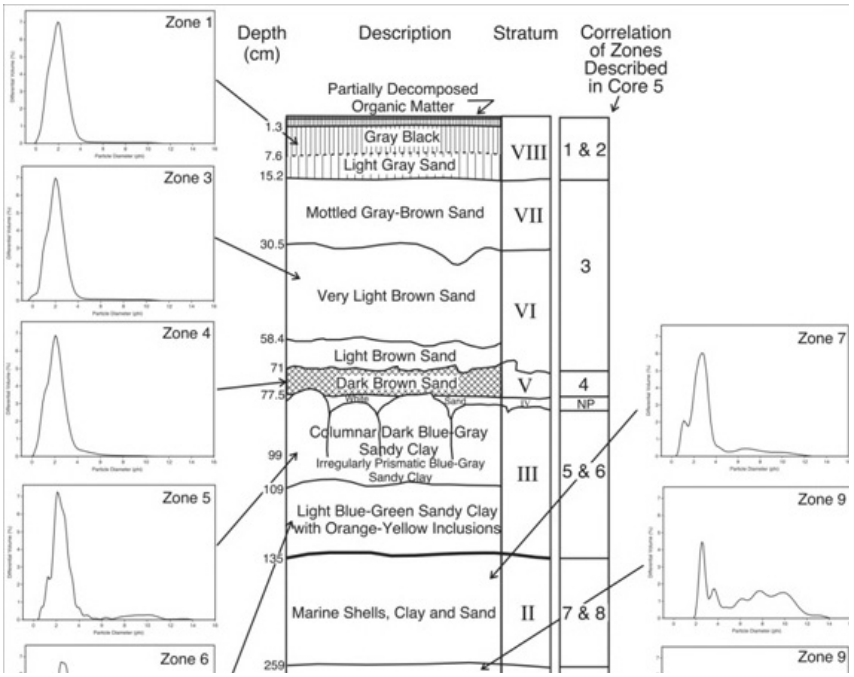

Figure 14. Edwards' stratigraphic description of the Helen Blazes Site (modified from Edwards 1954:25; Figure 4) is shown in the center of this figure with respect to sediment size histograms from various portions of the profile. Histograms plot Volume % on the Y-axis and grain size in phi on the X-axis. Left side of the diagram are samples derived from Edwards Strata III through VIII, which appear to represent the same Depositional Unit, whereas the histograms on the right side

gray (10YR 6.5/1) sand that decreases in organic matter and increases in hue with depth. This zone is the same as Edwards' Stratum VIIIB. A distinctly lighter colored but still slightly melanized zone was noted beneath the A-horizon between 18 and 25 cm depth, and was designated Zone 2. This light gray (10YR 7/1) sand was interpreted as a transitional horizon between the topsoil and the underlying eluvial horizon (an AE horizon) and correlates with Edwards' Stratum VIIIA. A 35-cm thick white (2.5Y 8/1) sand occurs between 25 and 60 cm and is interpreted as an E horizon that correlates with Edwards' Strata VI and VII. Edwards reports this portion of the deposit as almost twice as thick as was observed in this core and profile of HB2 from which the monolith was sampled (Edwards reports 56 cm vs. 26 cm in HB2 and 35 cm in Core 5). Figure 13, panel A, shows a photomicrograph of this horizon, which is subrounded to subangular quartz grains with little to no interstitial material and no grain coats. The E horizon rests upon a grayish brown (10YR 5/2) sand to loamy sand (Zone 4) interpreted as an accumulation of illuvial organic matter (a Bh horizon) formed during a period of spodic pedogenesis. This deposit has about the same amount of organic matter as the top of the A-horizon, but when viewed microscopically in thin section, clearly shows micro-features (specifically grain coats of illuvial organic matter) typical of Spodic Bh horizons (see Test 2, which shows the interface between the Zone 3 (the E horizon) and Zone 4 (the Bh horizon). Figure 12, panels B and C, clearly show grain coats of illuvial organic matter typical of Spodic Bh soil horizons.

Between 70 and 134 cm in Core 5 is a deposit that is gleyed and in the field exhibited prominent prismatic to columnar structure that clearly correlates with Edwards' Stratum III. This is the argillic horizon, comprising Zones 5 and 6. These zones are comosed of very dark grayish brown (10YR 3/2) loamy sand (the Btg1 horizon, Zone 5) and sand that graded into an underlying olive gray (5Y 5/2) to grayish brown (10YR 5/2) loamy sand and sand (Zone 6, the Btg2 horizon). Zone 6 contained common distinct fine to coarse yellowish brown (10YR 5/6) mottles. In the field this deposit exhibited prominent extremely coarse prismatic structure (peds ranging from 5 to 25 cm in diameter) where the ped margins were sharply delineated by very dark grayish brown (10YR 3/2) iron depletions up to 1-cm wide (Zone 5 in Figure 7). Zone 5 contains small amounts of clay and silt, but considerably more than the overlying sands, and was interpreted in the field as a Btg horizon. Examination of petrographic thin sections confirms the presence of illuvial clay coats in this deposit (Figure 13, panels D & E).

Zones 7 (the BCkg1 Horizon) and 8 (the BCkg2 horizon) comprise Edwards' Stratum II, and began at 134 cm and extended to 198 cm in Core 5. Zone 7 consisted of a light gray (2.5Y 7/2) to light olive gray (5Y 6/2) loamy sand that in places contained upwards of 40 percent marine shell and in other places contained upwards of 40 percent hard white nodules that were insoluble in hydrochloric acid, which Edwards identified as calcium phosphate, and a few small irregular-shaped calcium carbonate nodules. The shelly portions of this zone exhibited horizontal bedding but stratification was absent from the portions bearing nodules. Zone 8 ranged in color

from dark grayish brown (2.5Y 4/2) to greenish gray (10G 5/1) and in textures that ranged from silt loam to sand. Like Zone 7, this deposit contained several thin beds of marine shell and zones with carbonate and phosphatic nodules. Zone 9 (BCk3 horizon) occurred between 198 and 243 cm in the core and is clearly correlatedto Edwards' Stratum I. The deposit ranges from massive to thinly laminated, and the texture ranged from a silty clay to loamy sand. The matrix of Zone 9 was olive gray when fine textured and gray (10YR 6/1) when coarser. The significant increase in apparent organic matter in this deposit most likely represents structural water loss by clay minerals rather than organic matter.

Interpretation of Geological Events

Edwards interpreted Strata I through IV as shallow water marine sediments, the top of which (Strata III and IV) were subsequently altered by pedogenesis. A prominent period of erosion was identified between Strata III and IV. The sandy sediments that dominate the top of the profile (Strata V through VII) were interpreted as littoral sediments deposited adjacent to a freshwater lake or brackish water lagoon, and subsequently altered by podzolic pedogenic weathering. Stratum VIII was interpreted as the product of elevated water tables in the Late Holocene (after sea level and water table arrived at the present elevations).

Our interpretation of this profile differs significantly from Edwards and considers the majority of the sediments to have been originally deposited in a marine environment and significantly altered by post-depositional pedogenesis. Since Edwards' work, there has been considerable study of soils such as this that have bipartite profiles that are of significantly different texture and that are often referred to as texture-contrast soils (Phillips 2007). Debate concerning the origins of such soils typically revolves around whether the finer textured B horizons of the soil have been formed from illuviation of material stripped from the overlying sandy epipedon, or the two parts of the profile are inherently different depositional units, as Edwards interpreted.

Our first approach to addressing this issue employed the granulometric data generated from analysis of the monolith and the core. If the sandy upper portion of the profile was deposited in a different sedimentary depositional environment, it is likely that the sediments would exhibit significantly

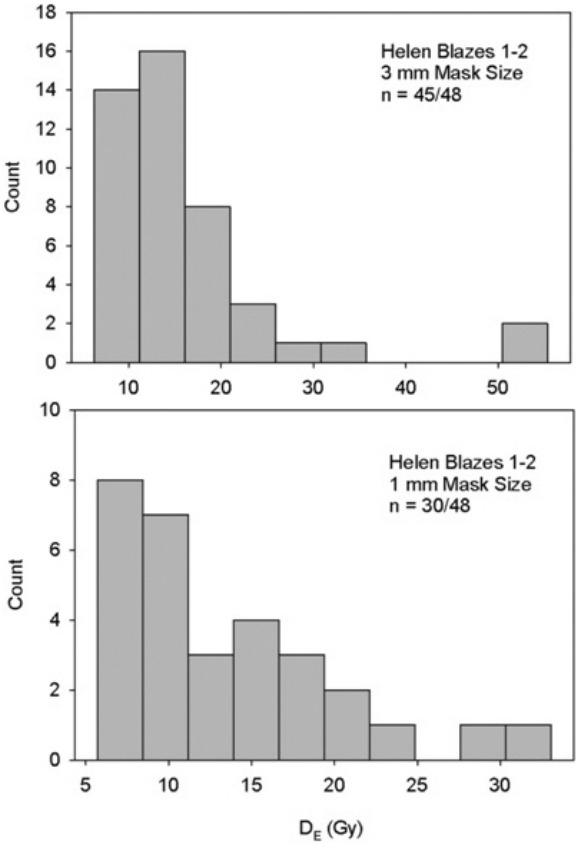

Figure 15. Equivalent Dose distributions for sample HB1-2 for two different aliquot sizes (3mm diameter aliquots = upper panel, 1mm diameter aliquots = lower panel). Value "n" is the number of aliquots which met criteria explained in methods section..

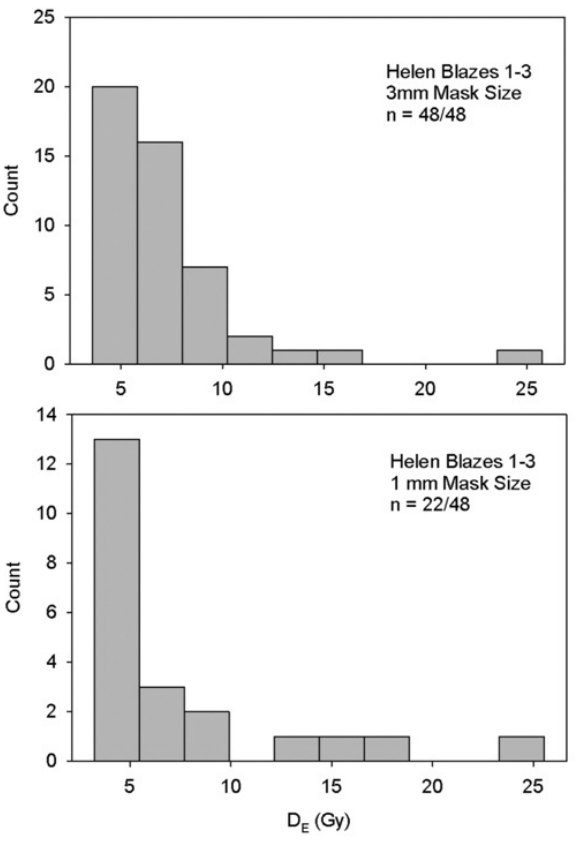

Figure 16. Equivalent Dose distributions for sample HB1-3 for two different aliquot sizes (3mm diameter aliquots = upper panel, 1mm diameter aliquots = lower panel). Value "n" is the number of aliquots which met criteria explained in methods section.

different granulometric attributes. Instead, the granulometric attributes of the deposits in Zones 1 to 6 (Edwards' Strata III to VIII) suggest that these sediments were created by the same sedimentary depositional process (see Figure 14). Although these sediments exhibit subtly different amounts of silt and clay, all are sand dominated and the sands are remarkably consistent, with a modal size between 2.027 and 2.028 phi. On the other hand, the deposits of Zones 7, 8, and 9 exhibit a range of different modal sand sizes, which are slightly finer textured and range between 2.1 and 3.1 phi. These sediments are also polymodal, much more so than the deposits in the upper portion of the profile that suggests more variable depositional processes. Hence, there appear to be two different sedimentary deposits here; the break is not where Edwards indicated but rather lower in the profile. The lower deposit, as Edwards convincingly demonstrates, is of a marine origin. There is no single attribute among the deposits of Zones 1 to 6 that firmly delineate the depositional environment (as do the marine shells in Zones 7 and 8, for instance), and Edwards considered the presence of fresh water sponge spicules in the very upper part of the profile (Zones 1 and 2; Strata VII and VIII) as indicative of a periodic inundation. But the presence of freshwater sponges in the A horizon does not necessarily mean the sands of the upper part of the profile were deposited in a freshwater setting as Edwards advocates.

Instead, we suggest that the entire profile was deposited in a marine environment during the last interglacial (most likely in two subtly different depositional settings). During the intervening glacial and interglacial periods these deposits were deeply weathered under two different climatic regimes, one associated with freely draining conditions that favored the formation of argillic horizons (Zones 5 and 6) and another that requires high water tables and periodic saturation in order for podzolization to occur. Several attributes of this profile support this model. First, the entire profile has been stripped of calcium carbonate to a depth of 135 cm (through Zone 6 or Edwards' Stratum III) and some of this carbonate was vertically translocated into Zones 7, 8, and 9 (Edwards' Strata I and II). Second, the development of prominent structure and the illuviation of clay in Zones 5 and 6 most likely occurred during the more arid periods of the last glacial, and the more hydric components of the profile (spodic pedogenesis [the Bh horizon Zone 4] and periodic inundation) occurred in the latter half of the Holocene since sea level reached its modern position. Evidence for the sequence of events may be found in micromorphologic examination of the very top of the Btg horizon (specifically at the interface between Zone 4 [the Bh horizon]; Edwards' Stratum V) and Zone 5 (the Btg, top of Edwards' Stratum III), where illuvial organic matter may be seen coating the outsides of illuvial argillans (Figure 13, panel F).

Edwards' observations on the presence of freshwater sponge spicules in Stratum VIII (the A horizon) and speculation on the presence of peat overlying the mineral soil that may have been removed prior to his work is consistent with this location being periodically inundated by standing water associated with Lake Helen Blazes on a seasonal basis. The incorporation of the sponge spicules into the mineral soil is consistent with ongoing pedoturbation, most likely during the dry season. We observed no evidence that would support delineating the A-horizon as a separate depositional unit given that it is virtually identical to the underlying sands.

The implications of this geological interpretation for the archeological deposits are significant in that the artifacts within the sandy portion of the profile have most likely been buried by pedoturbation rather than normal geological sedimentation.

OSL Dating Results

The OSL characteristics and dating results are shown in Tables 6 and 3, respectively. Table 3 shows that the main component of the total dose rates are the cosmic dose rates, which make up about 50 percent of the total dose rate. This makes the ages relatively insensitive to moisture content. There is some chance that even higher cosmic dose rates were experienced by the samples in early stages of burial, but we have no way of considering the magnitude of this possibility. In addition, there is always the possibility of some disequilibrium in the uranium decay chain because of the presence of acidic organic materials. However, the low concentrations of uranium in the sediments means that any disequilibrium would only have a minor effect on the uranium dose contributions.

We have calculated the ages using two moisture content values in an attempt to bracket the expected lowest and highest expected values that would have been present during the entire burial history. The lower sample (HB1-2, 37 cm below surface) shows an age range incorporating all uncertainties of 9000 to 12,000 years ago (thousands of calendar years ago), with most of the uncertainty in the individual estimates for this sample arising from the relatively large error in the equivalent dose. This sample corresponds to Stratum VIB of Edwards' diagrammatic section (Figure 3), but is constrained by correlation to Test 2 to be part of the lower portion of Stratum VI (Figure 12, lower panel). The upper sample (HB1-3, 20 cm below surface) yields a total age range of 5400 to 7000 years ago and corresponds to Stratum VI or lowermost Stratum VII (Figure 3), which we determined by correlation to the detailed sedimentological study at Test 2 (Figure 12, lower panel). The ages are statistically different from one another and in stratigraphic order.

Figures 15 and 16 show frequency histograms of the equivalent doses in all of the aliquots using two different aliquot diameters in each case. For the 3 mm and 1 mm aliquot diameters, the distributions in both samples show a strongly skewed distribution with many more aliquots showing younger doses. Because these distributions do not indicate a normal distribution of doses, and as discussed below, we believe the original deposition of grains occurred more than about 80,000 years ago, the only method to determine an apparent best age estimate is to assume that the minimum age model (Galbraith et al. 1999) is the best indicator, which we used in Tables 3 and 6. The minimum age model is designed to exclude higher dosed aliquot values in an attempt to isolate the distribution related to lower dosed aliquots, and thereby constrain the

calculated age to a younger value based on those lower-dosed aliquots.

If the grains had been incompletely zeroed at burial, we would expect a change from the 3 to 1 mm aliquot size that showed incorporation of larger doses as the aliquot size decreased, but generally we see no major changes in the distribution. However, we note that in the upper sample (HB1-3) we find the most strongly skewed distribution in the 1-mm size aliquot and relatively more low dose grains in this aliquot relative to the 3 mm aliquot (translating to younger age aliquots). Furthermore, when we compare the 1 mm aliquot between the two samples, we see that the upper sample (HB1-3) has a higher proportion of very young aliquots than the lower sample (HB1-2). We interpret these skewed distributions in both samples as a dilution of the best age estimate (carried by younger grains) by upwardly mobile older grains during the burial time. One possible way this can occur is by upward bioturbation of older grains by ants in a way that they do not reach the surface during ant transport, thus are not re-zeroed but carry the doses they received while buried deeper in the site. Similar processes were posited for OSL dating results at Wakulla Springs Lodge (Rink et al. 2012, this volume; Thulman 2012, this volume).

Discussion

The OSL age ranges reported are fully consistent with expectation based on artifacts that we recovered and some that Edwards found. In HB1 (from which the OSL samples came) we recovered a heat-treated flake at 19-20 cm depth (FS1 of Figure 11) and just below that depth, at 25-30 cm, a utilized flake (FS5 of Figure 11). The heat-treated flake is fully consistent with an age range of 5400 to 7000 years ago (HB1-3, 20 cm depth), generally considered to correspond to the Middle Archaic period in Florida in which heat treatment begins to appear in the archaeological record. Though none of our finds can unambiguously be assigned to the earlier Paleoindian period, Edwards did find diagnostic Paleoindian points distributed within Strata V and VI, which range in depth from 30-77 cm. We can assign an age of 9000 to12000 years ago at a depth range of 34.5 to 39.5 cm. This age range is fully compatible with the expected age range of the lanceolate points and point bases he recovered in these levels (Figure 13).

In general terms, how one interprets OSL age data depends on the sedimentary depositional process, the likely efficiency of that depositional process in resetting sand grains during transportation and the degree of post-depositional disturbance that has occurred. In this particular case, the lower part of the profile appears relatively undisturbed in that it retains depositional bedding and carbonate shells. But the OSL ages we obtained were not from this part of the profile, rather they were from the unstructured sands in the upper half meter. The absence of bedding and shells from this part of the profile, together with evidence of significant post-depositional alteration (e.g., a lack of bedding, vertical translocation of clay, and organic matter), indicates that these deposits have been significantly affected by post-depositional processes that may affect the OSL dating results. If, as we believe, the sediments at this site were deposited during the last interglacial, then a minimum age model would yield an incorrect age for the geological deposition of these sediments. But the likelihood of extensive disturbance by flora and fauna in addition to mechanical and chemical pedogenic processes means that the only age model that stands a chance of yielding the true geological depositional age would be a maximum age model, and the oldest aliquots obtained here would yield ages consistent with this interpretation (though such models are not at this point employed by OSL geochronologists). We see here that the micromorphology and grain size analysis support a model of extensive disturbance of a (depositionally) much older original sand host and find that the minimum age model seems to return results consistent with these observations. The only interpretive model that yields ages approximating the archeological inclusions is the minimum age model, and it does so by excluding old age aliquots in the primary data.

This interpretation turns a blind eye to the mixed grain age nature of this sandy deposit, but it also portrays a probable reality. Alterations of the age structure of the sand, following geological burial in a marine environment at this site have most likely occurred by upward exhumation of sand by insects, which in essence bury artifacts left on the ground surface and reset the grains in the process. This bioexhumation process has a net effect of "younging" the OSL age of the upper part of the soil profile, while simultaneously burying artifacts progressively deeper within the soil profile with increasing time. That the minimum-age model approaches the expected age of the artifacts reflects the resetting of the grains upon exhumation and their progressive burial as the bioexhumation process continues through time. So these ages do, in one sense, reflect burial of the artifact assemblage, although not by "normal" geologic deposition but by post-depositional internal re-organization of the deposit by the continuous actions of soil fauna such as ants.

Artifacts from the deepest component(s) of the site originated from depths of 30-52 cm that Edwards identified as the brown sands of Stratum VI (see Figure 3, also compare with Figure 12). The projectile points recovered from Helen Blazes in the 1950s include an array of different lanceolate and notched point forms. Elsewhere Edwards (1954:90) noted that "…. despite the vast variety of Paleoindian points in surface collections, it was found that single components at one site have a very limited number of highly specific point types, each of which appears thus to have spatial and temporal significance. The Helen Blazes point assemblage is thus not relatively limited but perhaps unusually varied." This was an important observation suggesting the Helen Blazes site might represent a multicomponent site that accumulated artifacts from more than one episode of occupation by temporally different Paleoindian toolmakers. However, there may be another explanation, that of a people in transition from a Paleoindian to Archaic lifeway.

For this possibility we must consider the artifact assemblage recovered from the late Paleoindian component at Dust Cave, Alabama. At Dust Cave human occupation was

impossible until sometime after about 12,485 cal B.P. because the cave was inundated prior to that time. After 12,485 cal B.P. the cave was occupied during the late Paleoindian period until about 11,400 cal B.P., after which a distinctive Early Archaic occupation took place. The late Paleoindian projectile point assemblage at Dust Cave consists of a highly varied group of lanceolate and side- notched point forms. The Early Archaic component, which the authors refer to as early side-notched, represents a classic Bolen point assemblage (Sherwood et al. 2004). It is possible that the diversity in lanceolate and notched point forms recovered by Edwards at Helen Blazes is similarly of late Paleoindian age. But until we have much tighter spatial and chronological control, it will be difficult to determine whether a site with a diversity of forms represents multiple occupations over a long time or captures the moment (or moments)) when people 'experimented' with different bifaces forms. The occurrence of small pressure flakes recovered in the window screen may also be important because Clovis and Simpson points are primarily reduced by percussion flaking, whereas waisted Suwannee and Bolen points are largely finished by pressure flaking. While the sample is small, if there were both pressure flakes and small percussion flakes, it would more strongly support a multicomponent occupation. With the information available it may be more likely that there is a single, late Paleoindian component followed by an Archaic component. The presence of a heat-treated chert artifact suggests that a firmer site age estimate could be obtained using thermoluminescence dating of the chert (if it turned out it had been heated sufficiently). However, with only a single piece of heated-treated chert, a high degree of confidence in the age would not follow.

Conclusions

A two-component archaeological sequence was identified at the Helen Blazes site. The upper component showed a heat-treated artifact consistent with manufacture in Archaic time, while the lower component yielded a core consistent with manufacture in either the Early Archaic or Paleoindian period. We interpreted the complex sedimentary sequence to have formed as a result of an initial stage of deposition of marine sands followed by a complex weathering scenario in the upper portions of the site. The OSL ages were similarly complex, in that a two-fold model for grain transport is posited: 1) a model of mixing of older grains (without zeroing) upward into younger levels, and 2) travel upward of grains to the surface (where they were zeroed) by bioturbation, A minimum-age model was employed to isolate the ages of the majority of grains that received zeroing by light exposure at the surface. Nevertheless the OSL age results are consistent with a period of geochemical change and bioturbation that was active in the interval from Paleoindian to Archaic times. The OSL data are consistent with the possibility that the artifacts themselves may have been buried by progressive pedoturbation and biomantling, rather than by deposition of sediments above them.

There are certainly other sites with seemingly equivalent, though undated strata that would benefit from more careful investigation. Such sites appear more frequent in the northern section of the St. Johns basin and include Silver Springs (Hemmings 1975; Hoffman 1983; Neill 1958, 1964) and the Lake George Point site (8PU1470; Thulman 2006, 2009, 2012 this volume). At Silver Springs, specifically the Paradise Park site, Neill (1958) collected artifacts from a borrow pit and from undisturbed contexts. Two Clovis fluted and unfluted Paleoindian points were found in the lowest levels (about 7 to 8 feet below ground surface [213-244 cm]). Neill proposed distinct living floors because the artifacts were lying flat in the sediments. The aceramic levels started at 48-54 inches (122-137 cm) and included Middle Archaic stemmed points. The Lake George Point site is characterized by more than 40 Suwannee-like points and broken lanceolate point bases, scores of unifacial chipped stone tools, and fossils of extinct fauna (Thulman 2006, 2009, 2012, this volume). Paleoindian materials in the southern reaches of the St. Johns are less well represented. Two other potentially early sites, Vero (8IR1) and Melbourne Golf Course (8BR44) are in this southern region, but remain problematic with respect to dating and association with the artifacts, human skeletal material and the Pleistocene megafauna (Berry et al. 1917; Gidley 1931; Sellards 1916).

Acknowledgements

The authors are most grateful to Dave Thulman for editing of the manuscript and to two anonymous reviewers for their comments. WJR thanks the Natural Sciences and Engineering Research Council of Canada for funding. We thank the Florida Public Archaeology Network for their generous support in the excavation work: specifically Dr. Rachel Wentz, Mr. Tim Brock and Mr. Nathan Lawers. We also are indebted to Ms. Beth Dykstra and Mr. Grayal Farr for extensive assistance in the field. We also are grateful to Mr. Bob Gross of the Florida Historical Society (Melbourne) for assistance in documenting Edwards' early work at the site. Field assistance in final survey work, establishment of permanent parkers and detail mapping was graciously provided by the Brevard Office of Natural Resources staff Gregory T. Jones and Susan Jackson.

References

Adamiec, G., and Aitken, M.J.
1998 Dose rate conversion factors: update. *Ancient TL* 16:37-50.

Berry, Edward Wilber, Oliver Perry Hay, Elias Howard Sellards, and Robert W. Shufeldt
1917 Additional studies in the Pleistocene at Vero, Florida. *Florida Geological Survey Special Publication*. Tallahassee.

Bullen, Ripley P.
1969 A Clovis fluted point from the Santa Fe River, Florida. *The Florida Anthropologist* 33:36–37.

Daniel, I. Randolph, and Michael Wisenbaker
1987 *Harney Flats: A Florida Paleo-Indian Site.* Baywood Publishing Company, NY.

Dunbar, James S.
1991 Resource orientation of Clovis and Suwannee age Paleoindian sites in Florida. In *Clovis origins and adaptation,* edited by R. Bonnichsen and K.L. Turnmire, pp. 185–213. Center for the Study of the First Americans, Oregon State University, Corvallis.

Dunbar, James S., and Pamela K. Vojnovski
2007 Early Floridians and late Mega-mammals: some technological and dietary evidence from four North Florida Paleoindian sites. In *Foragers of the terminal Pleistocene,* edited by Renee B. Walker and Boyce N. Driskell, pp. 167-202. University of Nebraska Press, Lincoln.

Dunbar, James S., and S. David Webb
1996 Bone and ivory tools from submerged Paleoindian sites in Florida. In *The Paleoindian and Early Archaic Southeast,* edited by D. Anderson and K. Sassaman, pp. 331–353. University of Alabama Press, Tuscaloosa.

Edwards, W. E.
1954 The Helen Blazes Site of Central-Eastern Florida: A study in method utilizing archeology, geology and pedology. Ph.D. dissertation, Department of Geology, Columbia University, New York.

Galbraith, R. F., R. G. Roberts, G. M. Laslett, H. Yoshida, and J. M. Olley
1999 Optical dating of single and multiple grains of quartz from Jinmium rock shelter,northern Australia: Part I, experimental design and statistical models. *Archaeometry* 41:339-364.

Gidley, J.W.
1931 *Further investigations of Early Man in Florida*. Smithsonian Institution, Washington, D.C.

Goodyear, A.C., III, and L. O. Warren
1972 Further observations on the submarine oyster shell deposits in Tampa Bay. *The Florida Anthropologist* 25:52–66.

Hemmings, E. Thomas
1975 The Silver Springs Site, Prehistory in the Silver Springs Valley, Florida. *The Florida Anthropologist* 28:141-158.

Hoffman, Charles A.
1983 A Mammoth Kill Site in the Silver Springs Run. The *Florida Anthropologist* 36:83-86.

Knight, Robert L.
2004 A comparative inventory of prehistoric lithic and bone tools found in five shallow gravel bars in the Middle Santa Fe River, Florida. *Amateur Archaeologist* 10:93–120.

Madsen, A.T., Murray, A.S., Anderson, T.J., Pejrup, M., and Breuning-Madsen, H.
2005 Optically stimulated luminescence dating of young estuarine sediments: a comparison with ^{210}Pb and ^{137}Cs dating. *Marine Geology* 214:251–268.

Means, Ryan C., and G. Harley Means
2004 Discovery of the Middle Paleoindian Ryan-Harley site, Wacissa River, North Florida. *Amateur Archaeologist* 10:35–42.

Murray, A.S., and A. G. Wintle
2000 Luminescence dating of quartz using an improved single-aliquot regenerative-dose procedure. *Radiation Measurements* 32:57-73.

Neill, Wilfred T.
1958 A Stratified Early Site at Silver Springs, Florida. The *Florida Anthropologist* 11:32-52.
1964 The Association of Suwannee Points and Extinct Animals in Florida. *The Florida Anthropologist* 17:17-32.

Phillips, J. D.
2007 Development of texture contrast soils by a combination of bioturbation and translocation. *Catena* 70:92-104.

Prescott, J.R., and J. T. Hutton
1988 Cosmic ray and gamma ray dosimetry for TL and ESR. *Nuclear Tracks and Radiation Measurements* 14:223-227.

Rink, W.J., Dunbar, James S., and Burdette, K.E.
2012 The Wakulla Springs Lodge Site (8WA329): 2008 excavations and new OSL dating evidence. *The Florida Anthropologist.*

Rouse, Irving
1951 A Survey of Indian River Archeology, Florida. *Yale University Publications in Anthropology 44*. New Haven, Conn.

Sellards, E.H.
1916 Human Remains from the Pleistocene of Florida. *Science* 44:615-617.

Sherwood, S. C., B. N. Driskell, A. R. Randall, and S. C. Meeks
2004 Chronology and Stratigraphy at Dust Cave, Alabama. *American Antiquity* 69:533-554.

Simpson, J. Clarence
1948 Folsom-like Points from Florida. *The Florida Anthropologist* 1:11-15.

Thulman, David K.
2006 A reconstruction of Paleoindian social organization in north central Florida. Ph.D. dissertation, Department of Anthropology, Florida State University, Tallahassee.
2008 A typology of fluted points from Florida. *The Florida Anthropologist* 60:165-178.
2009 Freshwater availability as the constraining factor in the Middle Paleoindian occupation of north-central Florida. *Geoarchaeology* 24(3):243-276
2012 Bioturbation and the Wakulla Springs Lodge Site artifact distributions. *The Florida Anthropologist* 65:23-34.

White, William A.
1970 The geomorphology of the Florida Peninsular. Florida *Geological Survey Bulletin No. 51*. Tallahassee.